Simple driven chaotic oscillators with complex variables

Delmar Marshall[1] and J. C. Sprott[2]
[1]*Department of Physics, Amrita Vishwa Vidyapeetham, Clappana P.O., Kollam, Kerala 690-525, India*
[2]*Department of Physics, University of Wisconsin, 1150 University Avenue, Madison, Wisconsin 53706, USA*

(Received 12 November 2008; accepted 21 January 2009; published online 5 March 2009)

Despite a search, no chaotic driven complex-variable oscillators of the form $\dot{z}+f(z)=e^{i\Omega t}$ or $\dot{z}+f(\bar{z})=e^{i\Omega t}$ are found, where f is a polynomial with real coefficients. It is shown that, for analytic functions $f(z)$, driven complex-variable oscillators of the form $\dot{z}+f(z)=e^{i\Omega t}$ cannot have chaotic solutions. Seven simple driven chaotic oscillators of the form $\dot{z}+f(z,\bar{z})=e^{i\Omega t}$ with polynomial $f(z,\bar{z})$ are given. Their chaotic attractors are displayed, and Lyapunov spectra are calculated. Attractors for two of the cases have symmetry across the $x=-y$ line. The systems' behavior with Ω as a control parameter in the range of $\Omega=0.1-2.0$ is examined, revealing cases of period doubling, intermittency, chaotic transients, and period adding as routes to chaos. Numerous cases of coexisting attractors are also observed. © *2009 American Institute of Physics*. [DOI: 10.1063/1.3080193]

It has become widely recognized that mathematically simple nonlinear systems can exhibit chaotic behavior. A logical question to ask is "How simple can a system be and still exhibit chaos?" Much of the work to date on this question has been on systems with real variables. This work asks the question for driven oscillators with complex variables. After a brief mathematical look at such systems, a search for simple examples is conducted. Seven systems found in the search are examined as to the degree of chaos present, i.e., the size of the largest Lyapunov exponent. The question of how these systems move into chaos, as a function of the driving frequency, is also investigated.

I. INTRODUCTION

Chaotic systems of equations with real variables have been and continue to be studied extensively,[1–5] but the study of chaotic systems with complex variables is a more recent pursuit. There have been numerous theoretical studies, particularly involving nonlinear oscillators, often with periodic forcing.[6–10] These systems have wide applications in physics, in areas as diverse as fluids, quantum mechanics, superconductivity, plasma physics, optical systems, astrophysics, and high-energy accelerators.[3,11–15]

Motivated by this more recent trend in research, and in line with previous work searching for simple systems of a given form that exhibit chaotic behavior,[16–20] this work began with a search for simple driven chaotic oscillators with a complex variable z, of the form $\dot{z}+f(z)=e^{i\Omega t}$. This form is equivalent, with $z=x+iy$ and $f(z)=u(x,y)+iv(x,y)$, where u and v are real functions, to the driven two-dimensional system,

$$\begin{aligned}\dot{x} &= -u(x,y)+\cos\Omega t,\\ \dot{y} &= -v(x,y)+\sin\Omega t,\end{aligned} \tag{1}$$

which can be recast as the autonomous three-dimensional system,

$$\begin{aligned}\dot{x} &= -u(x,y)+\cos\Omega t,\\ \dot{y} &= -v(x,y)+\sin\Omega t,\\ \dot{t} &= 1.\end{aligned} \tag{2}$$

There are numerous examples of driven two-dimensional systems that exhibit chaotic behavior.[5]

In Sec. II, some preliminary theoretical and experimental observations indicate why the search was expanded to systems with functions of the form $f(z,\bar{z})$. In Secs. III and IV, seven simple quadratic and cubic chaotic polynomial systems with real coefficients are examined, along with their behavior when Ω is used as a control parameter, including routes to chaos. Section V is a brief summary.

II. PRELIMINARY OBSERVATIONS

Excluding complex conjugates $\bar{z}$ most simple complex functions of z are differentiable by z except at isolated points, and so are analytic. Analytic functions obey the Cauchy–Riemann equations, $\partial u/\partial x=\partial v/\partial y$ and $\partial u/\partial y=-\partial v/\partial x$.

The Jacobian of system (2), assuming analytic $f(z)$ and using the Cauchy–Riemann equations, is

$$\begin{aligned}J &= \begin{bmatrix} -\frac{\partial u}{\partial x} & -\frac{\partial u}{\partial y} & -\Omega\sin\Omega t \\ -\frac{\partial v}{\partial x} & -\frac{\partial v}{\partial y} & \Omega\cos\Omega t \\ 0 & 0 & 0 \end{bmatrix}\\ &= \begin{bmatrix} -\frac{\partial u}{\partial x} & -\frac{\partial u}{\partial y} & -\Omega\sin\Omega t \\ \frac{\partial u}{\partial y} & -\frac{\partial u}{\partial x} & \Omega\cos\Omega t \\ 0 & 0 & 0 \end{bmatrix},\end{aligned} \tag{3}$$

which has eigenvalues 0 and $-\partial u/\partial x \pm i\,\partial u/\partial y$. The Lyapunov exponents (which measure the exponential rates of

separation of two nearby trajectories, and thus the degree of chaos) are the averages of the real parts of these eigenvalues along the trajectory: 0, $\langle -\partial u/\partial x\rangle$, and $\langle -\partial u/\partial x\rangle$. If the latter were both positive, nearby trajectories would separate exponentially in two directions, and so would have to be unbounded. Thus for bounded trajectories, any nonzero Lyapunov exponents must be negative: Nearby trajectories approach each other exponentially in two directions. The signature of chaos is sensitive dependence on initial conditions—nearby trajectories separating exponentially—so there can be no chaotic behavior for systems of the form $\dot{z}+f(z)=e^{i\Omega t}$, where f is analytic.

A simple way to alter the situation is to introduce the variable $\bar{z}=x-iy$. For a function $f(\bar{z})$, where $f(z)$ is analytic, the signs of the Cauchy–Riemann equations are reversed. The Jacobian becomes

$$J=\begin{bmatrix} -\frac{\partial u}{\partial x} & -\frac{\partial u}{\partial y} & -\Omega\sin\Omega t \\ -\frac{\partial v}{\partial x} & -\frac{\partial v}{\partial y} & \Omega\cos\Omega t \\ 0 & 0 & 0 \end{bmatrix}$$

$$=\begin{bmatrix} -\frac{\partial u}{\partial x} & -\frac{\partial u}{\partial y} & -\Omega\sin\Omega t \\ -\frac{\partial u}{\partial y} & \frac{\partial u}{\partial x} & \Omega\cos\Omega t \\ 0 & 0 & 0 \end{bmatrix}. \tag{4}$$

Thus for systems $\dot{z}+f(\bar{z})=e^{i\Omega t}$, the trace of the Jacobian is zero, i.e., they are area preserving, like Hamiltonian (roughly speaking, energy conserving) systems. A set of initial condition points (x_0, y_0) may change its shape, but the set will maintain its original area over time. However, for nonlinear $f(\bar{z})$, these systems cannot be Hamiltonian in the sense of having a mechanical analog because if $\dot{x}=y$, the reversed-sign Cauchy–Riemann equations mandate a *linear* system, the harmonic oscillator.

While we have not shown that systems of the form $\dot{z}+f(\bar{z})=e^{i\Omega t}$ cannot be chaotic, the observed behavior for polynomial $f(\bar{z})$ with real coefficients is that most trajectories diverge. In a few cases, there are stable limit cycles (the trajectory repeatedly cycles around a fixed, closed path) or tori (the trajectory remains on the surface of a torus). In two cases, a Poincaré section (a plot of y versus x at a chosen phase of the drive cycle, over many cycles), shows the torus breaking up into island chains for some values of Ω, as is commonly observed for a Hamiltonian system. With further changes in Ω, reduction in these cases, the trajectory begins to form a chaotic sea, but soon diverges. The basins of attraction (sets of initial conditions that end up on the attractor) are quite small, and it is the outermost of the nested tori that breaks up. With no stable, surrounding torus (a so-called KAM torus), there is no containment for the trajectory—it soon wanders outside the basin and diverges.

Given that analytic functions of z cannot produce chaos, and having found no polynomial functions of $\bar{z}$ with real coefficients that produce chaos, polynomial functions of the two variables z and $\bar{z}$ with real coefficients were introduced. Two obvious choices, functions of $(z+\bar{z})/2$ and $(z-\bar{z})/2i$, i.e., of x and y separately, were avoided because much work has already been done on finding simple examples of such systems[16–20] and because of the decision to restrict the search to polynomials with real coefficients.

III. QUADRATIC SYSTEMS

A search was conducted for the simplest chaotic quadratic polynomial $f(z,\bar{z})$ with real coefficients that displays chaotic behavior. The most general such quadratic function is

$$f(z,\bar{z})=a_0+a_1z+a_2z^2+a_3z\bar{z}+a_4\bar{z}+a_5\bar{z}^2. \tag{5}$$

The search assigned random coefficients a_i and used random initial conditions. The random values were taken from the squared values of a Gaussian normal distribution with mean zero and variance of 1, with the original signs of the values restored after squaring. For Ω, uniformly distributed random numbers between 0.1 and 2.0 were used. During the search, trajectories were followed using a fixed-step fourth-order Runge–Kutta integrator.[21] When a chaotic system was identified, an effort was made to simplify its coefficients a_i while retaining its chaotic behavior. The largest Lyapunov exponent was calculated using the method detailed in Ref. 5; there must also be a zero exponent, allowing the third to be obtained from the trace of the Jacobian.[5]

The three simplest chaotic quadratic systems (Lyapunov exponents for $\Omega=1$ in braces) our search method discovered were

$$\dot{z}+z^2-\bar{z}+1=e^{i\Omega t} \quad \{0.0473,0,-0.9869\}, \tag{6}$$

$$\dot{z}+(z-\bar{z})z+1=e^{i\Omega t} \quad \{0.0641,0,-0.2031\}, \tag{7}$$

$$\dot{z}+2z^2-\bar{z}^2+2=e^{i\Omega t} \quad \{0.0803,0,-0.0805\}. \tag{8}$$

The behavior of these systems with Ω as a control parameter was investigated; initial conditions for each system were kept constant at $(z_0,t_0)=(-0.5i,0)$. The investigation was conducted with a Cash–Karp adaptive-step fourth-order Runge–Kutta integrator,[21] which avoided numerical trajectory divergences observed with the fixed-step integrator in association with occasional large excursions from the chaotic attractors. Some of the changes in the attractors occurred with very small changes in Ω, so quite likely there are more to be discovered than those listed here.

A. System (6)

The attractor for system (6) is shown in Fig. 1. As Ω is reduced below 0.6, there is a limit cycle that adds a loop above the x-axis, then below, and so on, down to at least $\Omega=0.05$, where there are 26 loops, 13 above and 13 below. This phenomenon has been called period adding;[22] the limit cycle's overall period increases by one initial period at a time. If started from $z_0=-0.5i$, system (6) diverges at

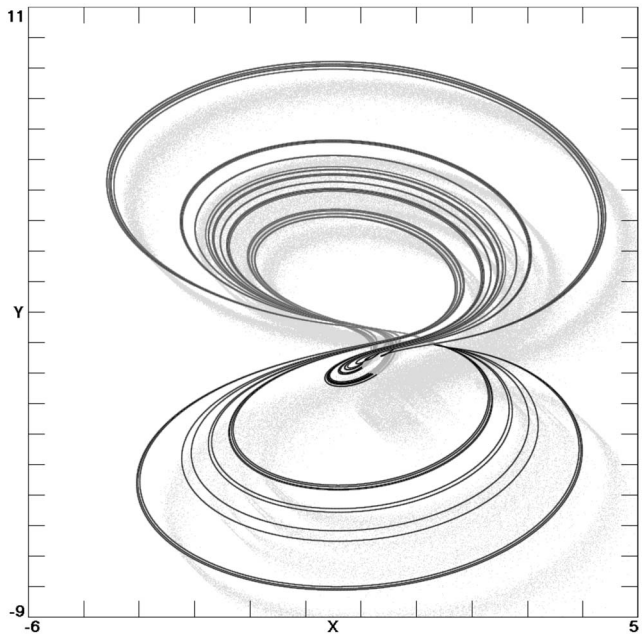

FIG. 1. Attractor for system (6).

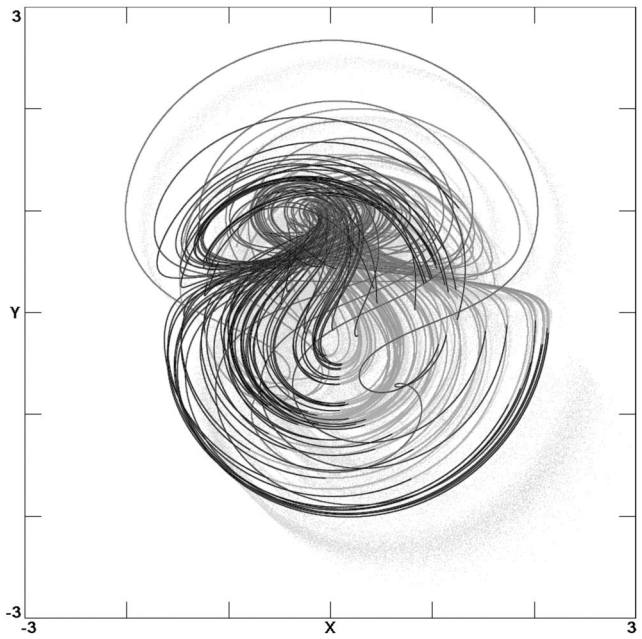

FIG. 2. Attractor for system (7).

$\Omega=0.54$, where a loop grows to infinite size as it flips from positive to negative y values.

From 0.6 to 0.85, there is a figure-8 shaped limit cycle similar to the figure-8 shaped strange attractor of Fig. 1. As Ω is increased from 0.85, the limit cycle period doubles (the limit cycle's period doubles repeatedly) three times to period 8 at 0.955, and then returns to period-4 before going chaotic near 0.959. The transition to chaos takes place by means of lengthening chaotic transients.

Chaos continues until $\Omega=1.023$, where the system produces a period-5 figure-8 limit cycle. This cycle period doubles to a narrow chaotic window in Ω values at 1.034. It reforms at 1.036, as a period-6 cycle, so the overall transition has been period adding. The sequence of period doubling to chaos followed by period adding continues, up to period 14 at 1.059, which then period doubles to a window of weak, intermittent chaos.

Increasing Ω further, intermittent periodic intervals lengthen, and then resolve into a limit cycle just above 1.064. This cycle, a single loop above the x-axis, grows ever larger with increasing Ω finally diverging at $\Omega=1.88$. Above 1.88, the loop returns, now below the x-axis, as observed at $\Omega=0.54$. The loop shrinks with further increase in Ω at least as far as $\Omega=2.3$.

B. System (7)

The attractor for system (7) is displayed in Fig. 2. For $\Omega=0.1$ upward, there is a limit cycle with varying-length chaotic transients. Competition between a torus and a limit cycle can be seen in some regions of Ω-space. Near 0.25, the torus prevails; but by 0.252, the limit cycle wins. At 0.253, there is an intermittent period-2 cycle with a pair of subcycles that separate into chaos. However, by 0.255, the subcycles come together into a period-1.

This sort of mix repeats in the intervals from 0.355 to 0.375, 0.45 to 0.49, 0.61 to 0.70, 0.82 to 0.85, and 0.89 to 0.92, with period-1 limit cycles in between. In some intervals, there are places where stable cycles either appear for certain Ω or form from the separating 2-cycle. With aslightly smaller Ω, there may be a weakly chaotic torus modeled on the 2-cycle. In Poincaré sections, the tori often appear as groups or chains of islands.

The interval between 0.89 and 0.92 differs from the others in two ways: A change in initial conditions suffices to recover the limit cycle; and coming out of the interval, a chaotic transient leads directly to the period-1 cycle, without intermittency. Above 0.92, the limit cycle becomes increasingly complex, finally period doubling between 0.954 and 0.955 to the chaotic attractor depicted in Fig. 2.

The attractor persists until, between $\Omega=1.22$ and 1.27, it reverse period doubles (i.e., its period is repeatedly halved) to a limit cycle. Limit cycles preceded by transients, at first chaotic, then almost periodic, continue as Ω is increased, although varying the initial conditions can result in either of two tori. Above 1.50, the chaotic transient is increasingly attracted to a weakly chaotic torus, which becomes established as an attractor by 1.56. The torus shrinks, then grows, stabilizes, and finally separates into islands above $\Omega=1.69$.

Above 1.70 the islands shrink, grow, and come together. The previous limit cycle returns above 1.78, through a chaotic transient. The torus then tries to gain the upper hand, resulting in a lengthening transient to a narrow window of chaos below 1.81. Coming out of this window via reverse period doubling, with chaotic transients, the torus forces a compromise: a figure-8 limit cycle at $\Omega=1.83$. The chaotic transient shortens at 1.84, lengthens again, and leads into chaos by 1.88. By 1.95, there is a torus composed of a group of islands, which shrink, grow, and come together as a simple torus by $\Omega=2.00$.

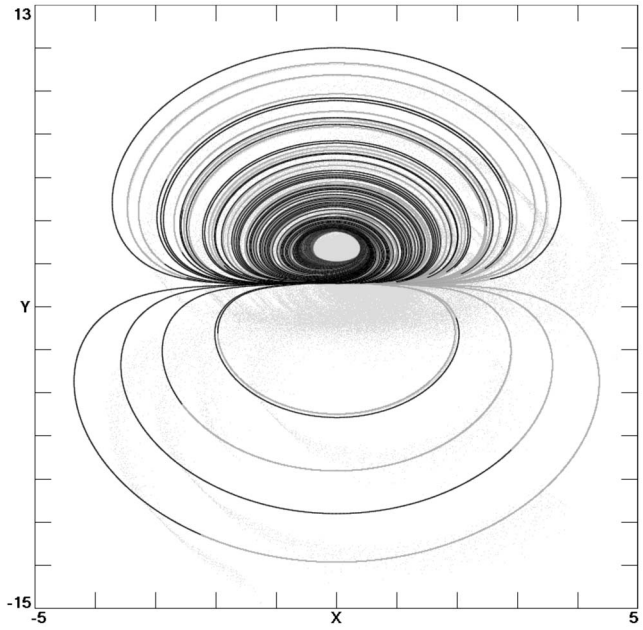

FIG. 3. Attractor for system (8).

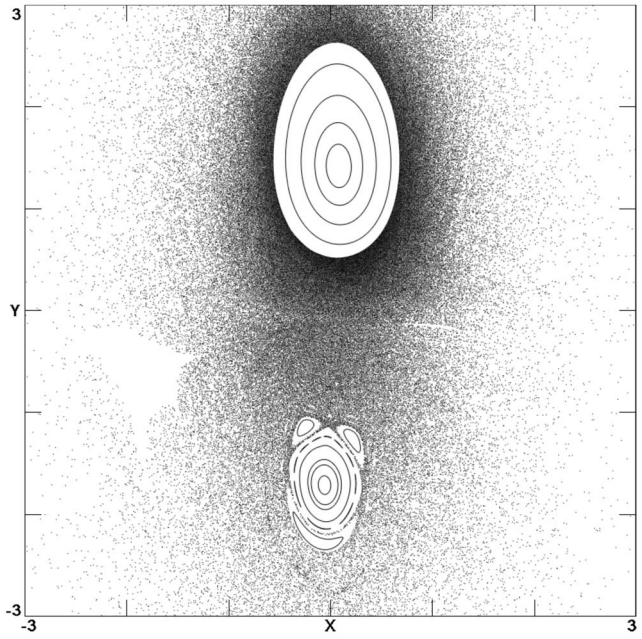

FIG. 4. Poincaré section for system (8), showing features typical of a Hamiltonian system.

In addition to those mentioned above, system (7) has other coexisting attractors. These exist for the same value of Ω but are reached from different initial conditions. For example, a trajectory that begins at $z_0=-1.5i$ is attracted to the single-loop limit cycle for any Ω between 1.3 and 1.8; to the figure-8 limit cycle for 1.85; and at 1.90 to a figure-8 torus of small islands, with a shape similar to the figure-8 limit cycle. From 1.95 to above 2.10, $-1.5i$ leads to chaos. The torus at $\Omega=1.70$ varies in shape as z_0 varies from 0 to $-i$.

C. System (8)

For system (8), Fig. 3 shows the attractor, evident for Ω between 0.1 and 2.0, although the chaos is weaker with smaller Ω, going through a minimum at 0.43. Above 1.0, the trajectory sometimes contracts onto a torus with weak chaos or no chaos; often these tori are composed of tiny islands when viewed in Poincaré sections. The contraction happens, for example, at approximately $\Omega=0.42-0.44$, 1.28–1.33, at approximately 1.40, and again at 1.98. The transitions can be rather sudden as a function of Ω.

A small change in initial conditions is sufficient to recover the chaotic attractor common to most values of Ω, so these tori are coexisting attractors. Other tori can be found by varying the initial conditions at values where the large attractor is seen for $z_0=-0.5i$. For example, $z_0=+0.5i$ produces a torus at $\Omega=1.0$. At $\Omega=1.1$, initial conditions from $z_0=-0.1i$ to $+5i$ produce a family of tori.

System (8) is almost area preserving; the trace of the Jacobian, the average of $-8x$ over the trajectory, is nearly zero: -1.8×10^{-4}. A Poincaré section of the trajectory starting from various initial conditions (Fig. 4) has all the features of a Hamiltonian system—a chaotic sea, KAM tori, heteroclinic trajectories (trajectories that connect saddle points), and island chains. Note, however, that the bulk of the chaotic sea resides outside the outermost KAM torus and is thus not contained. This is the same as the situation encountered earlier with the two cases of $\dot{z}+f(\bar{z})=e^{i\Omega t}$, which diverged after becoming chaotic. The difference here is that the basin of attraction is quite large, providing containment of the trajectory.

IV. CUBIC SYSTEMS

The search technique described in Sec. III was also used for cubic polynomial $f(z,\bar{z})$ with real coefficients. The resulting simplest four chaotic systems (Lyapunov exponents for $\Omega=1$ in braces) were

$$\dot{z}+0.3z^3+\bar{z}+0.3=e^{i\Omega t} \quad \{0.1231,0,-0.6053\}, \tag{9}$$

$$\dot{z}+(0.2z^2+1)z+\bar{z}=e^{i\Omega t} \quad \{0.1540,0,-1.3517\}, \tag{10}$$

$$\dot{z}+(z^2-\bar{z}^2)z+\bar{z}=e^{i\Omega t} \quad \{0.0892,0,-0.1621\}, \tag{11}$$

$$\dot{z}+(\bar{z}^2+z\bar{z}+z^2+1)\bar{z}=e^{i\Omega t} \quad \{0.1157,0,-6.1517\}. \tag{12}$$

Again the behavior of these systems with Ω as a control parameter was investigated, by the same method used for the quadratic cases, and using the same initial conditions for each system, $(z_0,t_0)=(-0.5i,0)$.

A. System (9)

The attractor for system (9) is displayed in Fig. 5. A limit cycle for $\Omega=0.1$ becomes chaotic at 0.3457, reverse period doubles to period-3 at 0.347, and moves through a narrow window of chaos to period-2 at 0.348. With increasing Ω, chaos returns, then gives way by shortening chaotic transients to period-3, back to period-2, and finally, by 0.351, back to period-1.

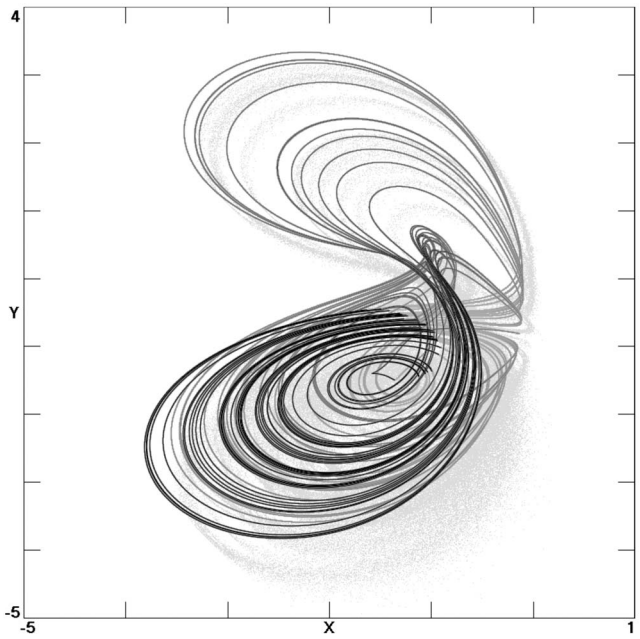

FIG. 5. Attractor for system (9).

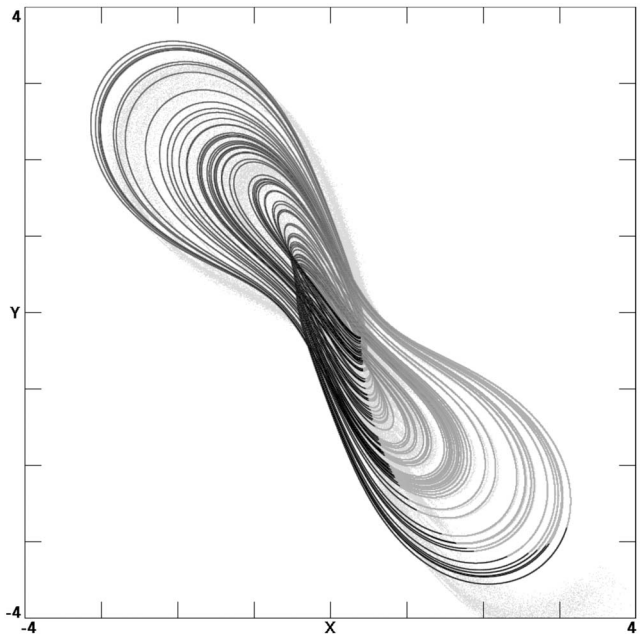

FIG. 6. Attractor for system (10).

The period-1 cycle breaks into chaos above 0.4095 and reverse period doubles back to period-1 by 0.422. The pattern repeats between 0.51 and 0.53, and again between 0.64 and 0.67. Just above 0.67, the system goes chaotic, until moving to period-6 and then to period-3 at 0.71. By 0.715, there is chaos again, which reverse period doubles to period-1 at 0.73. Transitions are gradual, with slow approaches to the final states. Except for a coexisting limit cycle that appears briefly at 0.77, the two-lobed limit cycle now bears a distinct resemblance to the two-lobed attractor in Fig. 5.

The limit cycle continues until $\Omega=0.89$, then moves into chaos at 0.9, through periods 2, 4, and 6, with slow approaches rather than sudden transitions. Chaos continues until, at $\Omega=1.07$ and 1.0825, there are limit cycles, with chaos in between. Above 1.0825, chaos reverse period doubles to period-1 near 1.11; transitions are through chaotic transients.

The limit cycle shrinks, but remains period-1, up to near 1.343, where it suddenly changes character and becomes substantially larger. The coexisting smaller cycle can be recovered from the initial condition $z_0=-0.2-0.5i$.

The larger cycle can also be reached at smaller Ω. From the initial condition $z_0=-0.4i$, just below $\Omega=1.09$ there is a transition from the smaller limit cycle to the coexisting larger one as a period-4. It period doubles to chaos at around 1.12, then reverse period doubles to period-1 at 1.21. It remains period-1 up to near 1.343, where it first appeared when starting from $z_0=-0.5i$.

Returning now to $z_0=-0.5i$: Above $\Omega=1.35$, the larger cycle develops a third and fourth lobes. From 1.42 to 1.45, there is a chaotic transient to the smaller limit cycle. At 1.46, the transient resolves into a cycle tracing just the third and fourth lobes of the four-lobed structure. This happens again at 1.48, but above and below 1.48, the smaller cycle is the result. At 1.58, the chaotic transient becomes long-term chaos, persisting until above 1.90. There the transient resolves into a large single-loop limit cycle, which shrinks with increasing Ω through at least $\Omega=2.00$.

B. System (10)

Figure 6 shows the attractor for system (10). For $\Omega=0.1$ to 0.888, there is a limit cycle, except for two narrow chaotic windows, from $\Omega=0.457$ to 0.463 and 0.467 to 0.479. Entry to the former window is by lengthening periodic transient and exit by reverse period doubling. Entry and exit to the latter are both by lengthening transient. From $\Omega=0.1$ to 0.48, the cycle has four lobes, although one lobe can be quite small. Above 0.48, it has two lobes, with the outline of the attractor of Fig. 6 beginning to form by 0.66.

At 0.8879, the two-lobed limit cycle adds an inner loop, becoming chaotic. After briefly stabilizing again at 0.8880, chaos continues, with the attractor increasing in size, up to $\Omega=1.31$. Above 1.31, the two-lobed chaotic attractor develops two more lobes, but reverts to a two-lobed limit cycle at 1.3522. The cycle period doubles to period 4 at 1.355, reverse period doubles back to period 1 at 1.358, then period doubles to chaos again just above 1.36. The resulting chaotic attractor has just two lobes at first, but with increasing Ω, soon recovers the other two. Chaotic transients of widely varying lengths lead into the limit cycles, where present.

The chaotic attractor continues to exist well beyond $\Omega=2$. With increasing Ω, the trajectory spends more time in a central helix formed from the inner loop that appeared at $\Omega=0.8879$, and less time in the outer loops that form the four lobes.

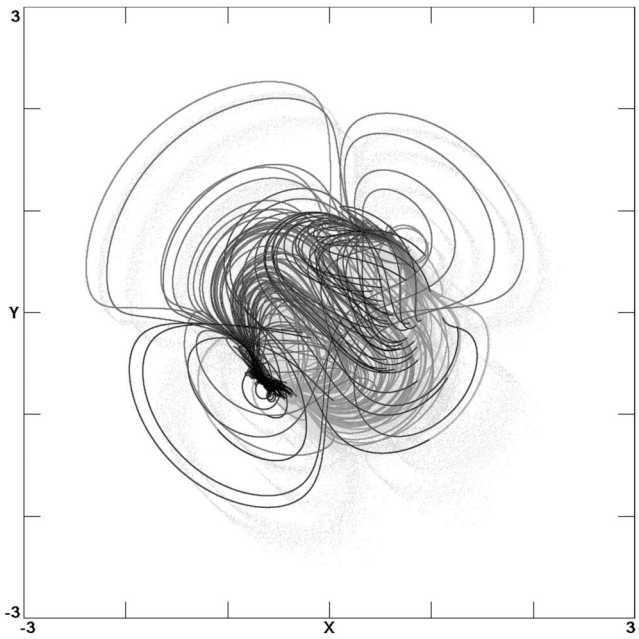

FIG. 7. Attractor for system (11).

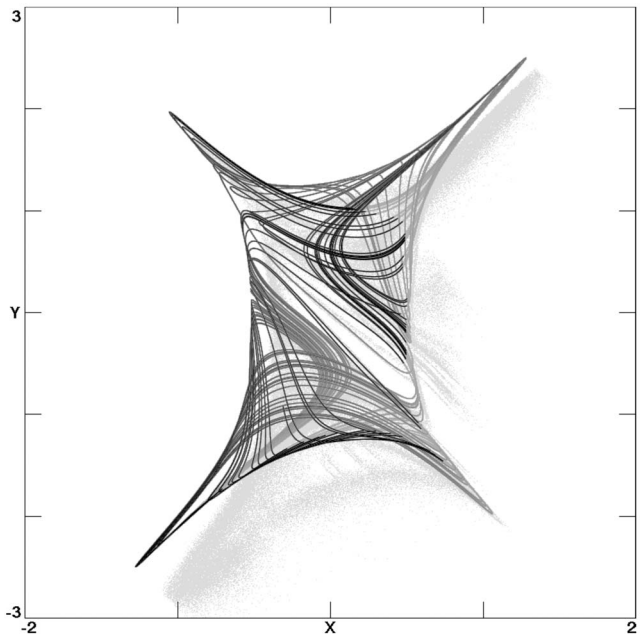

FIG. 8. Attractor for system (12).

C. System (11)

System (11) produces the attractor shown in Fig. 7. Note the symmetry, where sometimes x and y [i.e., Re(z) and Im(z)] change signs, flipping the attractor across the $x=-y$ line. This symmetry is also present in some of the limit cycles this system produces. There is hysteresis associated with the symmetry, since a chaotic trajectory can flip, but once established as a limit cycle, it cannot.

For this system, there exists a variety of limit cycles from $\Omega=0.1$ to 0.95, some very complex, and some with long chaotic transients, interspersed with narrow windows of chaos. Worthy of note is a 7-cycle at 0.65, which doubles to 14 and again to 28 before becoming chaotic below 0.651.

The chaotic window closest to 0.95 spans approximately 0.906–0.928. Entry is by intermittency; exit is by reverse period doubling. The resulting limit cycle at 0.9322 immediately period doubles back to chaos by 0.93 222.

This is the low side of a wide window of mainly chaotic behavior, with some closely confined exceptions: At 1.09, the chaos is very weak, and at 1.19 and 1.23, there are limit cycles. The wide window closes at $\Omega=1.243$, where a limit cycle forms again. This cycle persists until above 1.45, where a torus appears, first as a gradually lengthening transient; but finally taking over as an attractor, just above $\Omega=1.50$. Meanwhile, a symmetric pair of the previous limit cycles continues, coexisting with the torus.

The torus is a feature until 1.635, where it reclaims transient status, leading back to the limit cycle via a chaotic transient. At 1.64, the resulting limit cycle is quite distinct, but with further increase in Ω, the original version of the cycle soon reappears. By $\Omega=1.72$, there is again a chaotic attractor. Chaotic behavior continues until above $\Omega=2$; however, through $\Omega=1.90$, the torus can still be reached from $z_0=-0.7i$.

At 1.66, the initial condition $z_0=0$ leads to the distinct cycle noted at 1.64. Increasing Ω with this initial condition causes the cycle to become gradually more chaotic, until at 1.76 the resulting attractor is nearly indistinguishable from the one reached from $z_0=-0.5i$. Here is another case where the chaotic attractor seems to result from a contest between two different stable attractors.

D. System (12)

The attractor for system (12), shown in Fig. 8, displays symmetry across $x=-y$, like system (11). The limit cycles and chaotic attractors described below can exist on either side of the line or on both at once, depending on Ω and on the initial condition.

From $\Omega=0.1$ to 0.76, there is a limit cycle which, just above 0.76, period doubles to weak chaos. At 0.77 a narrow window for a period-5 cycle opens, while at 0.775 a narrow window begins for a period-3 cycle. Above the period-3 window, the system is chaotic, but at 0.84, a limit cycle reappears, period doubling back to chaos by 0.845.

At 0.86, a limit cycle exists in a very narrow range. Another limit cycle appears and disappears between 0.89 and 0.895; several more occupy the range between 0.895 and 0.902. From 0.903 to 0.906, there is weak chaos. At 0.907, a narrow window opens for a period-4 cycle, above which chaos prevails, until reverse period doubling leads to a limit cycle at 1.02. A lengthening transient leads to chaos at 1.03, followed by reverse period doubling to a limit cycle just below 1.05.

Intermittency then leads into chaos, out of it again by 1.12, and back in by 1.13. By 1.18, larger scale reverse period doubling begins, leading to a limit cycle just below $\Omega=1.30$. The transitions take place by means of a transient that gradually separates into a limit cycle. Then as Ω increases,

the transient gradually comes together into the next lowest period limit cycle. The resulting period-1 cycle at 1.30 persists until well above $\Omega=2$.

V. CONCLUSIONS

For complex-variable systems of the form $\dot{z}+f(z)=e^{i\Omega t}$, where $f(z)$ is an analytic function, it was shown that there can be no chaotic solutions. Furthermore, no chaotic solutions for systems of the form $\dot{z}+f(\bar{z})=e^{i\Omega t}$, with polynomial $f(\bar{z})$, were observed, but in a brief search for systems of the form $\dot{z}+f(z,\bar{z})=e^{i\Omega t}$, several simple chaotic systems were found.

With Ω as a control parameter, period doubling, intermittency, and lengthening chaotic transients as routes to chaos were observed in these systems, as well as period adding. In a number of cases, coexisting attractors occurred. Poincaré sections from some systems display characteristics of Hamiltonian systems, particularly in one case where the dissipation (energy loss) was very slight.

Further inquiries into chaotic complex-variable systems are planned.

[1]S. H. Strogatz, *Nonlinear Dynamics and Chaos with Applications to Physics, Biology, Chemistry and Engineering* (Perseus, Cambridge, 1994).
[2]J. Guckenheimer and P. Holmes, *Nonlinear Oscillations, Dynamical Systems, and Bifurcations of Vector Fields* (Springer-Verlag, New York, 1983).
[3]R. C. Hilborn, *Chaos and Nonlinear Dynamics* (Oxford University Press, Oxford, 1994).
[4]A. H. Nayfeh and B. Balachandran, *Applied Nonlinear Dynamics* (Wiley, New York, 1995).
[5]J. C. Sprott, *Chaos and Time-Series Analysis* (Oxford University Press, Oxford, 2003).
[6]G. Mahmoud and T. Bountis, Int. J. Bifurcation Chaos Appl. Sci. Eng. **14**, 3821 (2004).
[7]G. Mahmoud, A. A. Mohamed, and S. A. Aly, Physica A **292**, 193 (2001).
[8]Z. Xu and Y. K. Cheung, J. Sound Vib. **174**, 563 (1994).
[9]R. Srzednicki and K. Wójcik, J. Differ. Equations **135**, 66 (1997).
[10]K. Wójcik and P. Zgliczynski, Nonlinear Anal. Theory, Methods Appl. **33**, 575 (1998).
[11]G. M. Mahmoud, H. A. Abdusalam, and A. A. M. Farghaly, Int. J. Mod. Phys. C **12**, 889 (2001).
[12]V. A. Rozhanskiĭ and L. D. Tsendin, *Transport Phenomena in Partially Ionized Plasma* (Taylor and Francis, London, 2001).
[13]A. C. Newell and J. V. Moloney, *Nonlinear Optics, Reading* (Addison Wesley, Redwood City, 1992).
[14]D. Benest and C. Froeschlé, *Singularities in Gravitational Systems: Applications to Chaotic Transport in the Solar System* (Springer-Verlag, Berlin, 2002).
[15]R. Dilão and R. Alves-Pires, *Nonlinear Dynamics in Particle Accelerators* (World Scientific, Singapore, 1996).
[16]J. C. Sprott, Phys. Rev. E **50**, R647 (1994).
[17]J. C. Sprott, Phys. Lett. A **228**, 271 (1997).
[18]J. C. Sprott, Am. J. Phys. **65**, 537 (1997).
[19]J. C. Sprott and S. Linz, Int. Journal Chaos Theory and Appl. **5**, 3 (2000).
[20]J.-M. Malasoma, Phys. Lett. A **264**, 383 (2000).
[21]W. H. Press, S. A. Teukolsky, W. P. Vetterling, and B. Flannery, *Numerical Recipes in C: The Art of Scientific Computing*, 2nd ed. (Cambridge University Press, Cambridge, 1992).
[22]M. Levi, SIAM J. Appl. Math. **50**, 943 (1990).